

■ Organic & Supramolecular Chemistry

Anisotropic Nonlinear Optical and Optical Limiting Studies of an Ethylenediamminium Picrate Crystal with Femtosecond Excitation

Indumathi Chandrasekar,^[a, b] Alfred Cecil Raj Savari Rajan,^[b] Venugopal Rao Soma,^[c] Anitha Kandasamy,^[d] and Sabari Girisun Chidambaram^{*,[e]}

Femtosecond laser excitation (800 nm, ~150 fs, 80 MHz) induced anisotropic nonlinear optical behaviour and optical limiting action of ethylenediamminium picrate (EDAPA) crystal along two prominent orientations (2 0 0) and (1 1 1) was studied using the Z-scan technique. EDAPA exhibited reverse saturable type nonlinear absorption ascribed to two-photon absorption (2PA) process and self-defocusing based on nonlinear refraction. Intensity dependent nonlinear absorption studies portray the 2PA coefficient is independent of the peak intensity of excitation. Frontier molecular orbitals studies revealed the non-availability of real states at laser excitation (1.55 eV) and the measured energy gap of 3.18 eV avails the

energy states for simultaneous absorption of two photons involving virtual states leading to the occurrence of genuine 2PA. In addition, using molecular electrostatic potential (MEP) analyses polarizability (5.30×10^{-24} esu) and dipole moment (7.317 Debye) were calculated using the density functional theory. A variation in the NLO coefficients with respect to orientation of excitation arises due to the anisotropy of the crystal. EDAPA crystal along (1 1 1) orientation has high laser damage threshold (9.1 GW/cm^2) and low optical limiting threshold ($24.36 \mu\text{J/cm}^2$) and thus the wide dynamic range make it a preferred candidate towards laser safety devices for high repetition rate ultrashort laser pulse excitation.

1. Introduction

Since 1960, evolution of laser has been extraordinary and the necessity of improvising its unique characteristics (high intensity and coherence) has invented wide range of lasers from continuous wave to short pulsed to ultrashort pulse lasers. In particular, the peculiarity of ultrashort pulse lasers to deliver enormous amount of energy/density in short interval of time/space has compelled to consider ultrashort pulse lasers instead of conventional lasers that were already replacing the conventional light sources. Most importantly ultrashort pulse lasers with high-pulse repetition rate finds potential application in material processing, automobiles, photonics, semiconductors

and biomedical due to their special ability like rapid and localized energy deposition, precision and minimal stress load. Also, these femtosecond pulse lasers with megahertz repetition rates are utilized in optical sensors, fibre optic communications, nonlinear optical devices and frequency combs.^[1-3] Apart from the above mentioned less human interactive sectors, these lasers are nowadays used in hard tissue ablations like malignant tissue removal, orthopaedic surgery, oral malignancies treatment due to their ability to avail extremely precise ablation with minimal collateral (thermal and mechanical) damage.^[4,5] This have opened an alarming increase in the laser utilization which in turn resulted in the enormous laser accidents. This necessitates the need to develop proper laser safety devices that can give optical component protection from laser induced damage. Conventional optical filters that rely on linear optical properties are no longer useful for such high intense laser beams. Thus, passive optical limiting materials that do not obey Beer-Lamberts law to avail nonlinear extinction of being opaque at high intensity and transparent at low intensity are investigated all over the world.^[6,7] The development of optical limiters can be achieved through many nonlinear optical phenomena like reverse saturable absorption, two photon absorption, three/multi photo absorption, excited state absorption induced multiphoton absorption, self-focusing and defocusing, induced aberration, induced diffraction. Hence it is essential to understand the nonlinear optical behaviour of materials against high repetition rate ultrashort pulse lasers and develop laser induced nonlinear laser safety optical limiting devices.^[8,9]

[a] Dr. I. Chandrasekar
PG and Research Department of Physics, Bishop Heber College (Autonomous), Tiruchirappalli 620017, India

[b] Dr. I. Chandrasekar, Dr. A. Cecil Raj Savari Rajan
Department of Physics, St. Joseph's College (Autonomous), Tiruchirappalli- 620 001, India

[c] Prof. Venugopal Rao Soma
Advanced Centre of Research in High Energy Materials (ACRHEM), University of Hyderabad, Hyderabad 500046, Telangana, India

[d] Dr. A. Kandasamy
Department of Physics, Madurai Kamarajar University, Madurai 625021, India

[e] Dr. S. Girisun Chidambaram
Nanophotonics Laboratory, Department of Physics, Bharathidasan University, Tiruchirappalli 620024, India
Phone (Office): +91 (431) 2770136
Mobile: +91 - 98657 83510
E-mail: sabarigirisun@bdu.ac.in

Supporting information for this article is available on the WWW under <https://doi.org/10.1002/slct.201903269>

Earlier various organic NLO materials such as phthalocyanine, porphyrin-based derivatives were exhaustively investigated and carbonaceous materials like graphene have opened the opportunity to utilize aromatic structures for laser applications. Aromatic ring based molecules are interesting chromophores with one or more delocalized bonds which when substituted with donor and acceptor moieties induces large dipole moment. In the search for substituted ring like structure NLO chromophore, ethylene diamine substituted with different nitrophenols has yielded several interesting candidates like ethylenediaminium di(2-nitrophenolate), ethylenediaminium di(4-nitrophenolate), ethylenediaminium di(2,4-dinitrophenolate) and ethylenediaminium tri(2,4,6-dinitrophenolate) was recently reported.^[10–15] Among them, ethylenediaminium tri(2,4,6-dinitrophenolate) or ethylenediaminium picrate (EDAPA) with higher thermal stability against intense lasers and high third-order NLO coefficients was identified to be an entrant optical limiting material for safety devices against 532 nm in both CW (energy spreading, self-defocusing) and nanosecond pulses (energy absorbing, 2PA) laser radiation.^[14,15] Impressed by these facts along with the factor of possessing high linear transmittance in infrared domain, the extension of studying the optical limiting capability under the widely used Ti: Sapphire laser pulse (800 nm, 150 fs, 80 MHz) excitation. From device point of view, the measurement of the third-order NLO constants of EDAPA crystals in different plane of orientation was done for the possible realization of efficient optical limiters. For analysing the origin of NLO effect, quantum mechanical approach within a framework of the Density Functional Theory (DFT) was imposed to calculate the band structure.^[16–18] In recent years, theoretical estimation of NLO properties of complex organic molecules to establish the influence of individual moieties with aid of DFT calculation are under recent attraction. Various molecular structural parameters, molecular electrostatic potential map, charge transfer interaction and NLO property of various molecules were analysed by DFT method and using Natural bond orbital analysis.^[19–25] Notable report includes the establishment of role of halogen substituents in tuning the NLO properties of cycloparaphenylenes (CPP) and theoretical estimation shows high NLO values was obtained when one half of each CPP was substituted in halo CPP.^[19] The solvent-induced effects on the NLO of new pyrrole-pyrazoline derivatives were studied using self-consistent reaction field method in which increase in nonlinear absorption coefficient with solvent polarity was explained.^[20] The structural and electronic properties of imidazo^[1,5a] pyridine derivatives were evaluated at B3LYP/6-311 + G(d,p) level to elucidate their large Stokes shifts as well as NLO parameters in solvents of different polarities.^[21] The bell-shape behaviour of second hyperpolarizability of the asymmetric hetero-phenalenyl dimers was theoretically investigated and it was clarified by the new definition of diradical/ionic characters.^[22] Solvatochromic and computational investigations of linear and NLO properties of 2-(1,1-dioxidobenzo[b]thiophen-3(2H)-ylidene)malononitrile (BTD) was investigated using DFT calculations.^[23] A comprehensive study of linear and nonlinear optical properties of quinoxaline and its analogue Quinoline Yellow 54 was performed by

the Z-scan technique and DFT. It was reported that by a small structural change from CH to N atom in QY 54 core led to emissive analogue QY 54 A with enhanced ICT for better NLO properties.^[24] The intra-molecular charge transfers from natural bonding orbital analysis of newly synthesized NLO material ethyl4-(3-(1,3-dimethyl-1H-pyrazole-5-carboxamido) phenyl)-1,2,3,4-tetrahydro-6-methyl-2-oxopyrimidine-5-carboxylate was made using TD-DFT calculations.^[25] Thus combined theoretical and experimental approach can shed more light upon the possible utilization of EDAPA crystals as optical limiters against the highly challenging femtosecond near-IR pulse lasers.

2. Results and Discussion

2.1. Preparation and Confirmation

The preparation of title compound aims to create a push-pull mechanism through a proton transfer between a donor and acceptor groups, to avail a strong delocalized NLO system with high NLO coefficient. In the employed acid-base reaction, ethylenediamine reacts with picric acid in methanol environment to yield yellow microcrystalline powders.^[10,14,15] Highly pure EDAPA powders obtained through grinding of crystals were subjected to powder X-ray diffraction (PXRD) study employing PANALYTICAL XPERT-PRO powder diffractometer equipped with Cu K α radiation at a wavelength $\lambda = 1.5405 \text{ \AA}$ for preliminary confirmation. The diffraction recorded over the 2θ range of $5\text{--}50^\circ$ at rate of $1^\circ/\text{min}$ was detected using a scintillation detector. To avoid the error deviation in recorded experimental and simulated XRD, crystal that was utilized to record single crystal XRD (CIF data used for simulation of powder XRD) was grounded and used for recording experimental powder XRD. The observed diffraction peaks were indexed effectively using POWDER X software. Figure 1 depicts the indexed, experimentally recorded PXRD pattern and the corresponding theoretical PXRD pattern of EDAPA simulated using MERCURY 3.7 software.^[18] The sharp Bragg's peaks at specific 2θ angles establishes the good crystalline nature and quality of the EDAPA microcrystalline powders. The major strongest peak of orientation observed in experimental and simulated PXRD pattern of EDAPA was (0 0 6) plane. It is to be mentioned that even though the strongest peak comes close to (6 2 0), based on the calculated intensity it was indexed as (0 0 6). The similarity of pattern and matches found in indexed peak ascertained the formation of EDAPA microcrystalline powder. The slight mismatch in the peak position and peak intensities of recorded experimental powder XRD arises mainly due to hidden diffraction intensities that arises from transformation of single-crystal diffraction (3 dimensional) data into powder diffraction (1 dimension) data. Similar observation through comparative single-crystal and powder XRD crystal structural determination of griseofulvin was reported by PAN QingQing et al.,^[26] Further the obtained XRD pattern was analysed by using Autox software package and lattice parameters were evaluated. The evaluated cell parameters are $a = 21.918 \text{ \AA}$; $b = 15.396 \text{ \AA}$; and $c = 19.816 \text{ \AA}$ and the results agree very well with the reported values.^[14] Table 1 shows the

Table 1. Comparison of lattice parameters of EDAPA obtained from PXRD and SXRD.

Cell Parameters	PXRD	SXRD ^[14]
a (Å)	21.918(2)	21.920(5)
b (Å)	15.396(6)	15.398(5)
c (Å)	19.816(5)	19.828(5)
System	orthorhombic	orthorhombic

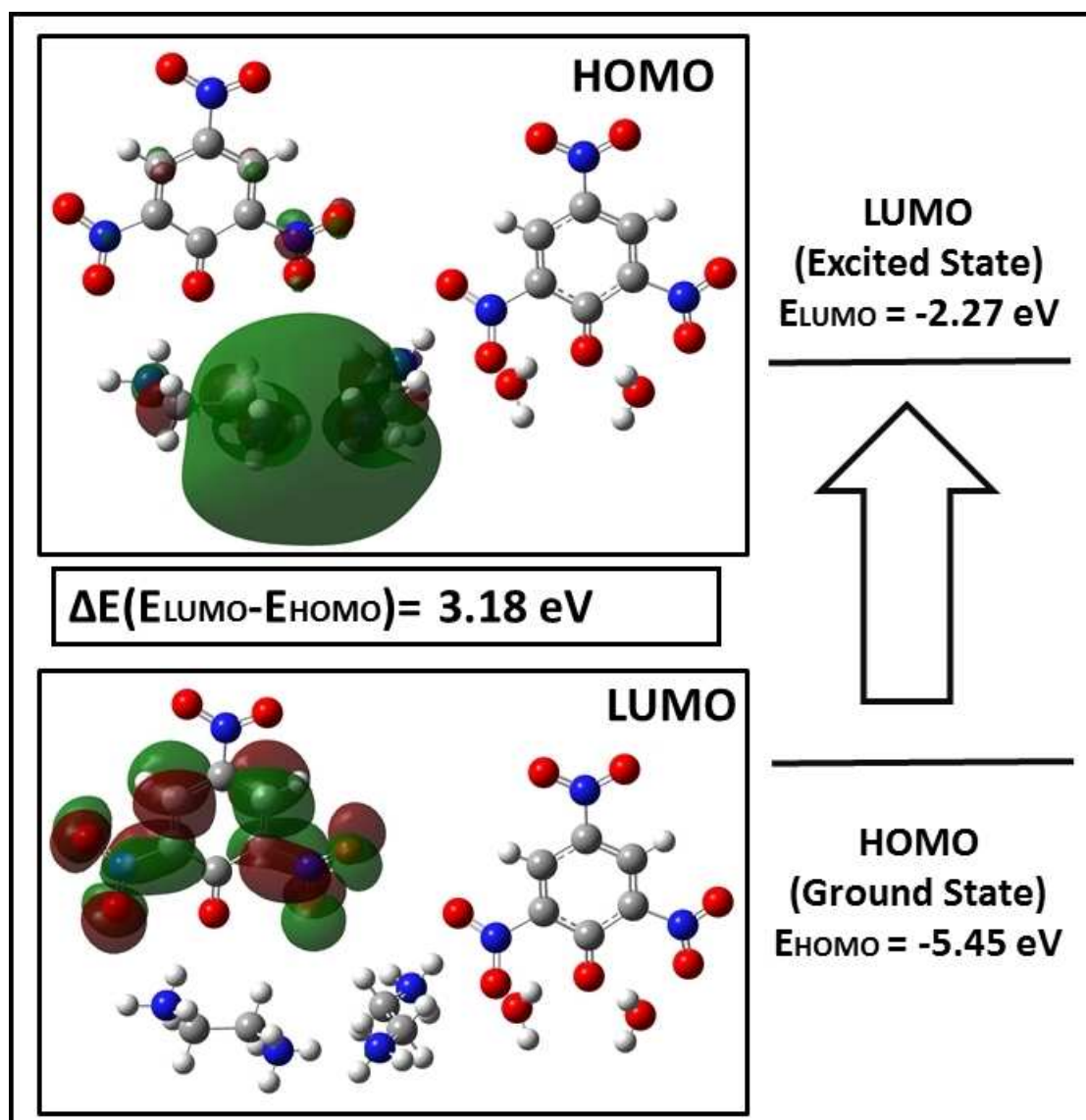


Figure 3. HOMO and LUMO orbitals of EDAPA molecule with iso-value of 0.02 a.u.

crystal possesses high chemical reactivity as well as high polarizability. Chemical hardness defines the chemical stability and reactivity of a molecule. Soft molecules possess small energy gap and are highly reactive, while hard molecules with large energy gap are highly stable and need higher energy for molecular excitation. Furthermore, electronegativity (power of a molecule to attract electrons onto itself) and can be obtained from Koopman theorem using the value of HOMO and LUMO.^[27–29] The chemical hardness ($= -\frac{1}{2} (E_{\text{HOMO}} - E_{\text{LUMO}})$) and

electronegativity ($= -\frac{1}{2} (E_{\text{HOMO}} + E_{\text{LUMO}})$) of EDAPA were obtained as 1.59 eV and 3.86 eV respectively. These properties suggest that EDAPA could be a promising material for NLO applications and in particular the measured energy gap of 3.18 eV avails proper energy state for two photon absorption under IR laser (800 nm, 1.55 eV) excitation.

3.2. Molecular Electrostatic Potential (MEP)

The molecular electrostatic potential is generally associated with the electron density, which plays a crucial role in determining electrophilic and nucleophilic reactive sites and hydrogen bonding interactions of a molecule.^[30,31] The reactive sites and molecular interaction investigation is helpful in understanding the drug–receptor system in biological and pharmaceutical applications. In order to predict the electrophilic and nucleophilic reactive sites, iso-electron density is mapped with molecular electrostatic potential surface and is represented in Figure 4. The most electronegative and positive electrostatic potentials regions are signified by red and blue colour shades, respectively. The positive electrostatic potentials were found over the NH_3^+ groups of both ethylenediamine cations and which are recognized nucleophilic attack sites. Whereas negative electrostatic potentials were localized over the oxygen atoms of two nitro groups attached to the picrate anion and monohydrate moiety and these regions are acknowledged as electrophilic attack sites.

3.3. Combined NLO Properties Calculations

3.3.1. Theoretical Estimation: *Ab Initio*

Theoretical estimation of NLO parameters of EDAPA was estimated through finite-field approach. Materials used for the potential electro-optic device and NLO applications must possess large first-hyperpolarizability value. The nonlinear optical properties such as dipole moment, polarizability and first hyperpolarizability of a compound depends on its structure. *Ab-initio* calculations provide a valuable approach towards investigating the structure-property relationships. The understanding of the microscopic origin of nonlinearity helps to investigate macroscopic NLO properties of a molecule. This is a preliminary level test that can throw light on the capability of a material to be used as NLO material, most importantly as optical limiter against intense laser pulses. In the presence of electric field, NLO properties such as dipole moment (μ_α), polarizability ($\alpha_{\alpha\beta}$), first-order hyperpolarizability (β) components were calculated for the title compound (Table 2), using Taylor series expansion of the energy.^[16,17]

When applying the weak and homogenous electric field, the energy arises

$$E = E^0 - \mu_\alpha F_\alpha - \frac{1}{2} \alpha_{\alpha\beta} F_\alpha F_\beta - \frac{1}{6} \beta_{\alpha\beta\gamma} F_\alpha F_\beta F_\gamma \quad (1)$$

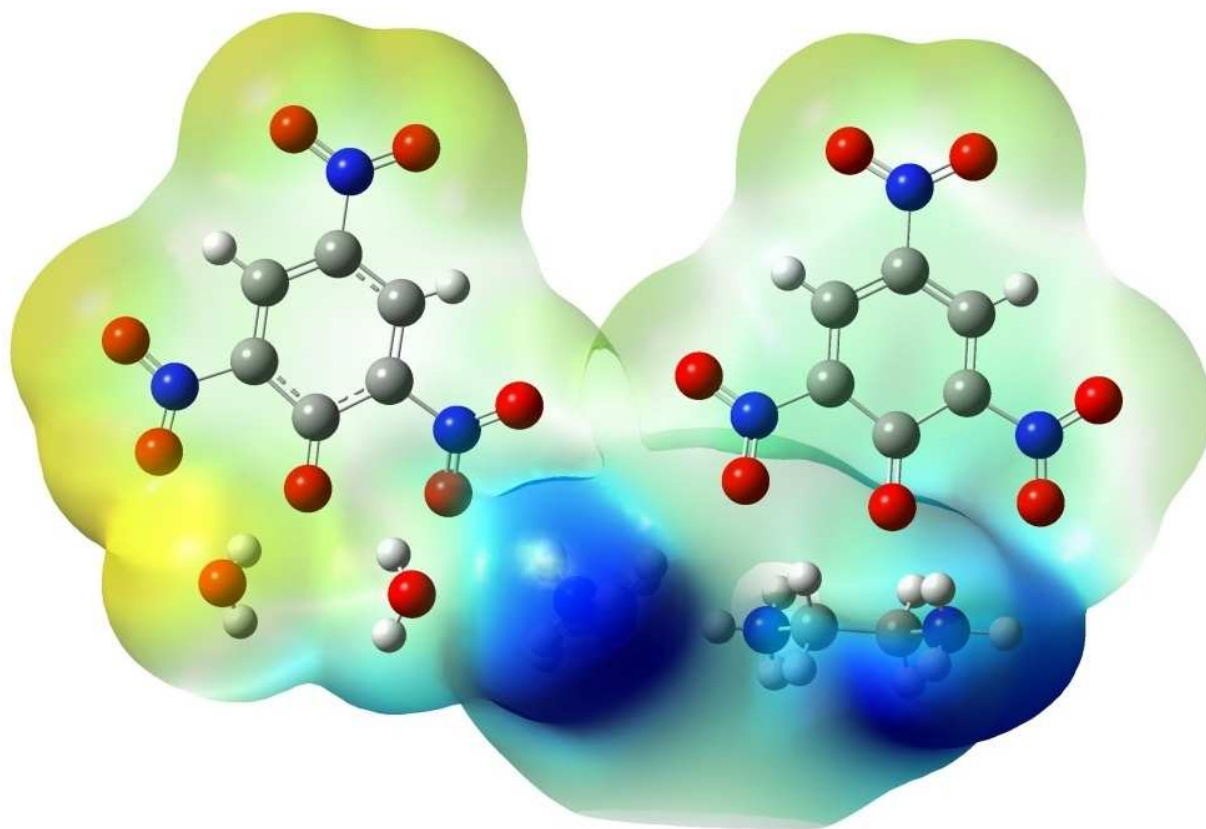


Figure 4. Molecular electrostatic potential surface of EDAPA with iso-value of 0.0004 a.u and the potential increases in order of red < orange < yellow < green < blue.

Table 2. Calculated electric dipole moment, polarizability and first hyperpolarizability components calculated at B3LYP-6311++G(d,p) for EDAPA.

Dipole moment (Debye)	α components (10^{-24} esu)	β components (10^{-33} esu)
μ_x 7.191	α_{xx} 1.0737	β_{xxx} 84.865
μ_y -1.280	α_{xy} 0.037	β_{xxy} -85.840
μ_z 0.435	α_{yy} 8.478	β_{xyy} 8.289
μ_0 7.317	α_{xz} -1.251	β_{yyy} 13603.53
	α_{yz} 1.107	β_{xxz} 75.554
	α_{zz} 6.348	β_{xyz} 315.345
	α_0 5.300	β_{yyz} 4243.159
		β_{xzz} 21.260
		β_{yzz} 1149.176
		β_{zzz} 205.042
		β_{total} 15349.09

where E^0 is the energy of the unperturbed molecules, E is the energy of a molecule in the presence of applied the electric field F and F_α is the electric field at the origin. The mean first order hyperpolarizability β_{total} is calculated using x , y and z -components,

$$\beta_{total} = \sqrt{\beta_x^2 + \beta_y^2 + \beta_z^2} \quad (2)$$

Where $\beta_x = \beta_{xxx} + \beta_{xyy} + \beta_{xzz}$; $\beta_y = \beta_{yyy} + \beta_{xxy} + \beta_{yzz}$ and $\beta_z = \beta_{zzz} + \beta_{xxz} + \beta_{yyz}$

The average dipole moment (μ_0) and polarizability (α_0) are calculated from the most general formulation

$$\mu_0 = \sqrt{\mu_x^2 + \mu_y^2 + \mu_z^2} \quad (3)$$

$$\alpha_0 = \frac{\alpha_{xx} + \alpha_{yy} + \alpha_{zz}}{3} \quad (4)$$

The β_{yyy} component of the hyperpolarizability value shows the largest value, which indicates the direction of electron delocalization. The calculated first hyperpolarizability (β), polarizability (α_0) and dipole moment (μ_0) of EDAPA are 15.349×10^{-30} esu, 5.30×10^{-24} esu and 7.317 Debye. EDAPA possess non-zero dipole moment and definite polarizability which confirms the non-polar nature and microscopic origin for NLO behaviour. The obtained higher total static dipole moment shows the stronger intermolecular interactions involving the van der Waals type dipole-dipole forces. Dominance of the longitudinal components of hyperpolarizability, β_{yyy} , β_{yyz} and β_{yzz} indicates large delocalization of charges in these directions. The first hyperpolarizability of EDAPA is found to be 30 times greater than well-known organic NLO reference material (urea with a value of 0.512×10^{-30} esu). These results further suggest that EDAPA can be an entrant material for future NLO applications.

3.4. Experimental: Z-Scan Measurement

Experimental estimation of third-order NLO coefficients and nonlinear absorption can be effectively determined by open and closed aperture Z-scan measurement. In the choice of laser

excitation source, mode-locked Ti: Sapphire (wavelength of 800 nm) femto second (pulse duration of 150 fs) laser pulses (Chameleon, coherent) delivered at a high repetition rate of 80 MHz was used. This is because the delivered laser pulses possess very high peak intensity (MW/cm^2) that can induce interesting higher-order of nonlinear absorption and repetition rate involved offers thermal nonlinearity as well in the system. In the employed experiment, the input beam with beam waist ($\omega_0 = \frac{2f\lambda}{\pi D}$) of $25.5 \mu\text{m}$ was focused using a plano-convex lens (focal length, $f = 100$ mm) on the sample whose input energy was controlled using neutral density filters. Along the direction of focused beam, EDAPA crystal with (1 1 1) and (2 0 0) as orientation plane of excitation was moved using a translation system and its corresponding far-field output transmittance was measured. Here for each chosen orientation, optical quality crystals of thickness 1 mm (path length) was cut and polished and is maintained to be less than Rayleigh range ($Z_0 = 2.54$ mm) to satisfy thin-medium approximation. For a various input power of 3–9 mW, the corresponding peak intensity ($I_0 = \frac{2P}{\pi\omega_0^2}$) was estimated to be 245–735 MW/cm^2 . For both orientations, experiments were repeated several times at different spots in the crystal and the best data were taken for analysis.^[32,33]

The recorded open aperture pattern at peak intensity of 245 MW/cm^2 for EDAPA crystals with two different orientation (1 1 1) and (2 0 0) plane of excitation is displayed in Figure 5. It shows strong valley pattern where the transmission of the sample is maximum at the wings and minimum at the focal point. This confirms the presence of reverse saturable absorption in the EDAPA crystal and there is a noticeable change in the depth profile pattern where the nonlinear absorption is altered with change in the orientation plane of irradiation. Nonlinear absorption is broadly classified as: resonant nonlinearity that involves slow actual transitions and non-resonant nonlinearity that is fast involving virtual transitions. Single photon and excited state absorption are the predominant mechanism in the resonant region, while it is a genuine multi-photon absorption processes in the non-resonant region. Therefore, depending on the materials property observed sign and magnitude of the nonlinearity changes.

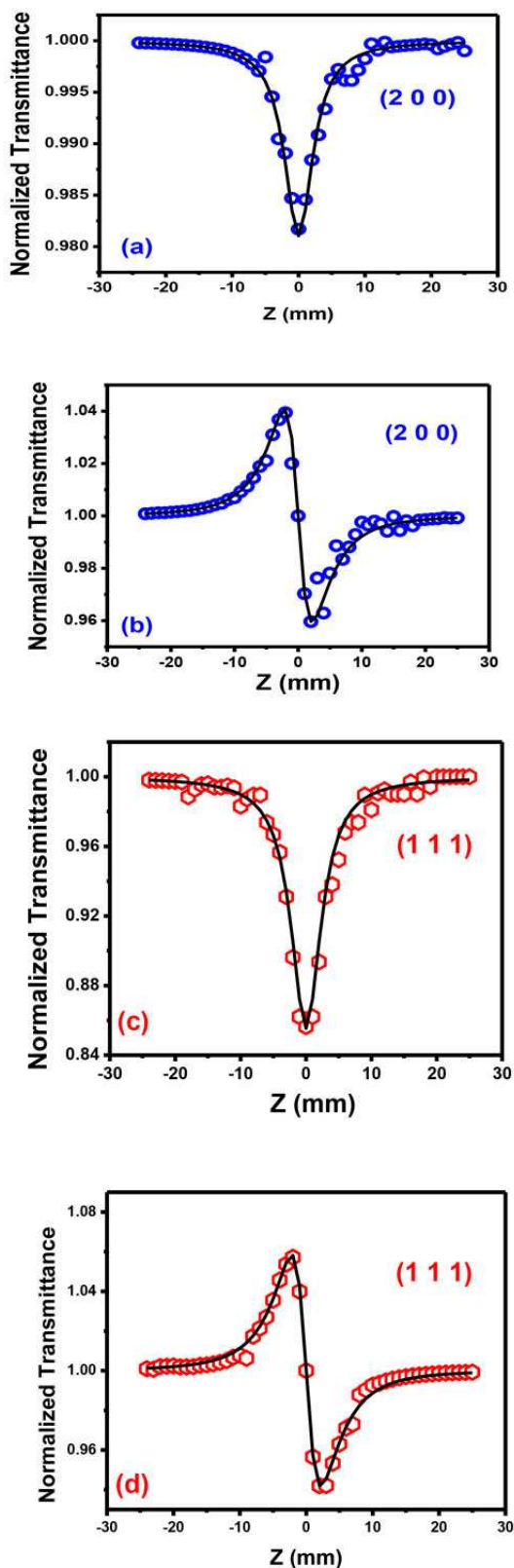


Figure 5. OA and CA Z-scan pattern of EDAPA Crystal along (2 0 0) and (1 1 1) orientation

Under fs laser excitation, the observed nonlinearity may arise due to NLO mechanisms like saturable absorption, reverse saturable absorption (RSA), two-photon absorption (2PA), three-photon absorption (3PA) and excited state absorption (ESA). To understand the nonlinear absorption process of EDAPA crystal the acquired data were fitted using the standard relation for open aperture normalized transmittance. The open circle indicates the recorded experimental data and the solid lines correspond to the theoretical fit which was found to be best fitting for two-photon absorption process. Furthermore, it is well known that 2PA process can take place when the laser energy is larger than half of the band gap of the material ($h\nu > E_g/2$).^[34] As discussed in the molecular orbital analysis, the HOMO-LUMO bandgap of EDAPA was estimated to be 4.1 eV and thus it satisfies the condition for 2PA process.

A proper theoretical fit made between experimental and numerical data assures the reliability of experiment and it does not shed any light on the nature of 2PA as genuine 2PA or sequential 2PA. To understand the exact nature of involved process, intensity dependent nonlinear absorption of EDAPA crystal was studied at different excitation input intensity of 245–735 MW/cm². The acquired data were fitted using the standard relation for open aperture normalized transmittance and change in the nonlinear absorption coefficient with respect to input intensity can provide information on the mechanism involved. Genuine 2PA occurs when β value remains constant for varied input intensity as weak 2PA cannot drain the population of electrons in the ground state. However, in ESA process due to substantial depletion of ground state population nonlinear absorption coefficient either will increase or decrease as function of peak intensity. Here for EDAPA crystal with both orientations, 2PA coefficient was found to be almost constant with various input peak intensities, which ascertain the occurrence of genuine 2PA. Further as depicted in the molecular orbital analysis, EDAPA crystal possess negligible absorption at 800 nm which is the excitation wavelength domain and hence the observed nonlinearity is expected to be of non-resonant type. Non-availability of real states at 1.55 eV compels the process of simultaneous absorption of two photons involving virtual states leading to the occurrence of genuine 2PA. The involved mechanism in the observed nonlinearity of 2PA can be explained as follows: Under NIR (800 nm) laser excitation, electrons cannot undergo one photon absorption due to the non-existence of energy states at 800 nm, 1.55 eV. So electrons in the HOMO (ground state, -5.45 eV) level absorbs two photons through simultaneous process and transit to the of LUMO level (excited state, 2.27 eV) of EDAPA crystal. Here energy gap of EDAPA crystal (3.18 eV) avails energy state to accommodate two photon absorbed excited (1.55 eV + 1.55 eV) electrons and thus the involved nonlinear absorption is verified to be genuine 2PA.

Nonlinear refraction arises generally due to electron transition nonlinearity, reorientation effect or thermal lensing effect or mixture of them. As the laser chosen for excitation possess high repetition rate (80 MHz), contribution of thermal effects is unavoidable and hence the EDAPA crystal will suffer nonlinear refraction. Involved nonlinear refraction process and

nonlinear refractive index of the material can be evaluated by closed aperture Z-scan experiment. The recorded closed aperture pattern at lower intensity ($I_0 = 250 \text{ MW cm}^{-2}$) of excitation is shown in Figure 5. The experimental data were found to be fitting well with the theoretical estimation from closed aperture normalized transmittance data. In the recorded closed aperture pattern the circles represent the experimental data and the lines correspond to the theoretical fits. The CA Z-scan of EDAPA crystal in both orientations was found to exhibit a peak-valley configuration, characteristic of self-defocusing behaviour, i.e., negative nonlinear refraction. The nonlinear refractive index (n_2) value was obtained by fitting the normalized transmittance versus the sample position with the theoretical equation. Estimated nonlinear optical coefficients of EDAPA crystal in two orientation is summarized in Table 3. The obtained values clearly shows that the orientation of crystal plays a vital role in deciding the strength of nonlinearity. Variation in NLO coefficients arises due to the anisotropy of the crystal and here (1 1 1) orientation show almost one order of magnitude higher values than (2 0 0) plane.

High repetition rate femtosecond lasers are utilized regularly in hard tissue ablations and in laser-based microsurgery. For controllable photochemical damage with such lasers the intensity threshold is $\sim 3 \times 10^{11} \text{ W/cm}^2$ and thus safety measures of using passive optical limiters to control fluence in the order of $\mu\text{J/cm}^2$ is ultimately required. Onset optical limiting threshold is the input fluence point at which the output intensity starts deviating from nonlinearity. From open aperture Z-scan, the input laser energy density was evaluated using the standard relation. The position dependent fluence was evaluated using the standard relation. Figure 6 shows the extracted optical limiting pattern of EDAPA crystals in both orientations. The solid lines indicates the theoretical fit and the curve reveals under strong fluence the curve departs from Beer's law, i.e., nonlinearity leading to optical limiting behavior. The mechanism for optical limiting is due to the 2PA and moreover the curve depth indicates the higher limiting behavior. EDAPA with (1 1 1) plane possess low limiting threshold ($24.86 \mu\text{J/cm}^2$) than other (2 0 0) orientation ($45.67 \mu\text{J/cm}^2$). Also, the limiting threshold of EDAPA was found to be lower than other limiting materials like Duran glass and ZnO thin films irradiated with similar laser.^[3,16] Thus it is clear that EDAPA crystal along (1 1 1) orientation which has high nonlinear absorption coefficient, nonlinear optical susceptibility and low onset optical limiting threshold can be a preferred candidate for high power optical

Crystal Orientation	Nonlinear absorption coefficient (10^{-10} m/W)	Nonlinear refractive index ($10^{-16} \text{ m}^2/\text{W}$)	NLO Susceptibility ($10^{-18} \text{ m}^2/\text{V}^2$)	Onset optical limiting threshold ($\mu\text{J/cm}^2$)
(1 1 1)	8.1	1.40	1.78	24.86
(2 0 0)	0.85	0.12	0.14	45.67

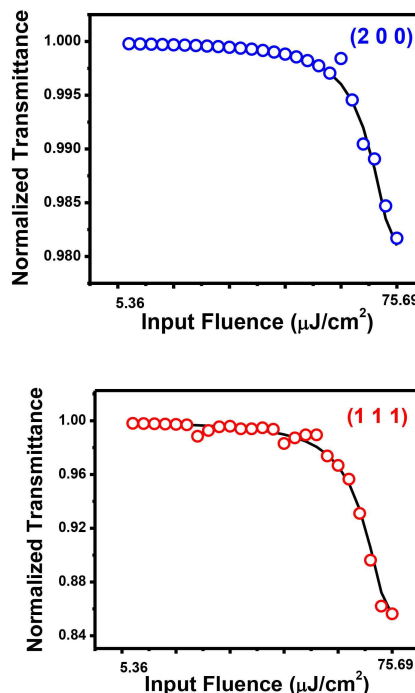


Figure 6. OL pattern of EDAPA Crystal along (2 0 0) and (1 1 1) orientation

limiting applications with ultrashort laser pulse (800 nm, 150 fs) excitation.

3.5. Photoconductivity and Dielectric Studies

In order to ensure the reliability of EDAPA crystal for device performance as optical limiter, it is essential to understand the photoconductivity and dielectric loss of the material. Photoconductivity study was carried out on grown crystal by using a Keithley 6517B electrometer. The opposite faces of polished crystal were silver painted using electronic grade silver paste and a two thin copper wire was connected on the both sides of the crystal. Then the crystal was connected in series with DC power supply. The input voltage was increased from 10 V to 100 V. The crystal was prevented from all the radiations and resultant dark current was recorded. The photo current was measured by illuminating the crystal with 100 W halogen lamp with iodine vapour and tungsten filament. Figure 7. depicts the dark current Vs photocurrent for the EDAPA crystal with applied voltage. It shows that dark current is higher than photo current and this phenomenon is called negative photoconductivity. It may be decrease of charge carriers in the presence of external radiation.^[27] The negative photo conducting nature suggest that EDAPA crystal can be very much useful for IR detector applications and optical limiter for NIR lasers.^[35] The materials that exhibit low dielectric constant and loss at higher frequencies can be employed in electro-optic applications such as DAST and optical limiters.^[36] The dielectric studies were measured for grown EDAPA crystal using Hioki 3535–50 LCR

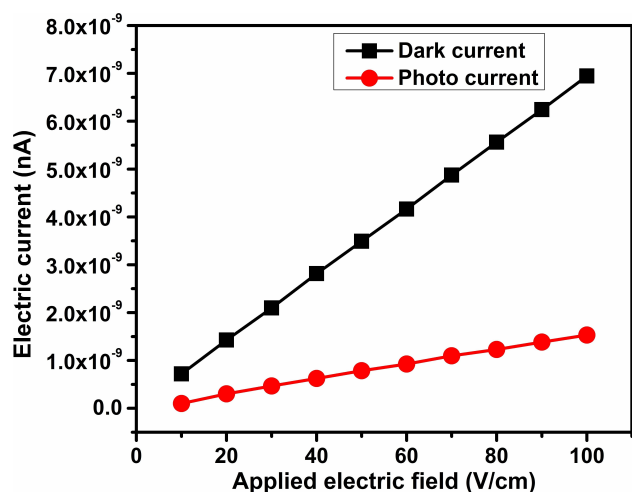


Figure 7. Photo conducting response of EDAPA crystal along (1 0 0) orientation.

HITESTER in the range from 50 Hz to 5 MHz at different temperatures. A parallel capacitor has been designed by placing the grown crystal between two copper electrodes. Figure 8a. represents the variation of dielectric constant (ϵ_r) of EDAPA crystal as a function of frequencies with different temperatures 303 K, 327 K and 347 K. It is seen that with increasing frequency, the dielectric constant (ϵ_r) decreases at a constant temperature. The dielectric constant occurs due to the contribution of four distinct polarizations such as electronic, dipole orientation, ionic and space charge polarizations. At low frequencies, the dielectric constant of EDAPA crystal was found to be high, which is corresponding to the existence of space charge polarizations. This polarization arises due to the low power dissipation and reflects the purity and perfection of materials. Figure 8b. represents the variation of dielectric loss

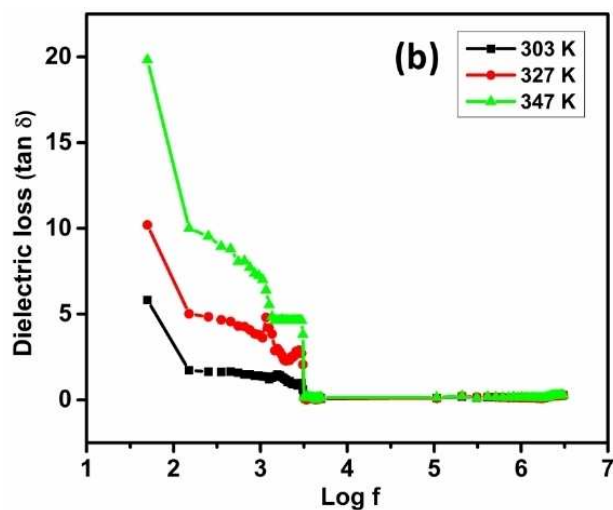


Figure 8. (a) Dielectric constant Vs log f and (b) Dielectric loss Vs log f at 303, 327, 347 K temperatures.

as a function of frequencies with different temperatures 303 K, 327 K and 347 K. It is noticed that with increasing frequencies, the dielectric loss decreases due to the charged lattice defects.^[37] Both dielectric constant (ϵ_r) and dielectric loss ($\tan \delta$) decrease with increasing frequencies at constant temperatures, which make this crystal suitable for electro-optic and photonics applications.^[38]

3.6. Microhardness and Laser Damage Studies

Investigation on mechanical stability and laser damage studies shed light on the possible utilization of EDAPA crystal as laser safety device. The microhardness of EDAPA crystal was analysed by Vicker's microhardness test. The test was performed on EDAPA single crystal on the (1 1 1) plane (which possess higher NLO performance) using Shimadzu HMV Vicker's microhardness tester fitted with a diamond pyramid indenter. Indentations were made on the crystal gently by the applied loads (P) 25, 50, 75 and 100 g for a dwell period of 10 s. Crystals suffered multiple cracks beyond the load 100 g due to the release of local internal stresses generated by indentation. Using a calibrated micrometer attached to the eyepiece of the microscope, the length of the two diagonals was measured. For every load, at least five well-defined impressions were considered and the average of all the diagonals (d) was taken. The Vicker's hardness number was calculated using the relation, (kg/mm^2).

The variation of microhardness number with the applied load is plotted in Figure 9. The plot depicts that H_v increases with load, which reveals that the crystal exhibits reverse indentation size effect (RISE). Existence of distorted zone, effect of vibrations, near crystal-medium interface, radial cracks, specimen chipping etc., may contribute to the observed RISE.^[39] Based on Meyer's law ($H_v = kP^{-n}$), a plot made between $\log P$ and $\log d$ is shown in Figure 10. The plot is more or less a straight line and from the slope, the Meyer's index or work hardening coefficient (n) was calculated as 3.5. According to Onitsch and Hanneman, the value of ' n ' lies between 1 and 1.6 for hard

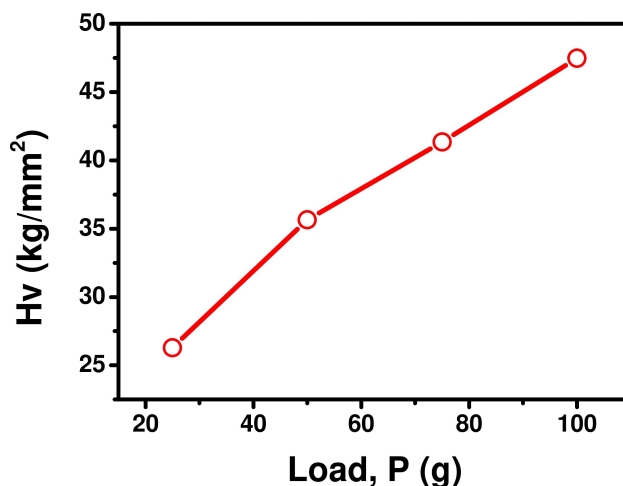


Figure 9. Load Vs Hardness number of EDAPA crystal with (1 1 1) orientation

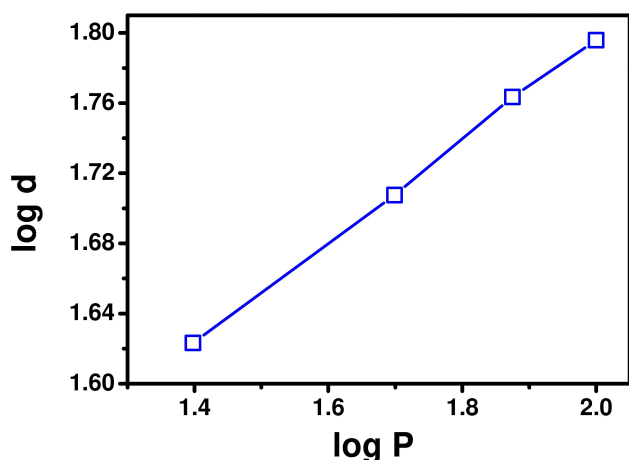


Figure 10. log P Vs log d of EDAPA crystal with (1 1 1) orientation

material and above 1.6 for soft material. Hence from the value of work hardening coefficient, the EDAPA crystal was categorized as soft material with reverse indentation size effect. Further, the standard hardness (k_1) coefficient was estimated from the intercept ($\log k_1$) of the straight line. The value of k_1 can also be obtained from slope of the plot d^n vs P (not shown here) and the values in both the cases was found to be 6.3×10^4 kg/m. By Hays and Kendall's theory of resistance pressure (W), there is a minimum level of resistance pressure (W), below which no plastic deformation occurs. The plot of d^2 vs d^n is a straight line having a slope k_2/k_1 and intercept W/k_1 (Figure 11). Knowing already the value of k_1 , the values of another hardness constant (k_2) and resistance pressure (W) are estimated as 3.5×10^7 kg/m and 0.9 g respectively. Also using Wooster's empirical formula, the elastic stiffness constant was calculated as 3 GPa, which shows the tightness of bonding between the neighbouring atoms.^[40]

Multi-shot laser induced surface damage studies were carried out using the second harmonics of Q-switched Nd: YAG laser (1064 nm, 10 ns, 10 Hz). The (1 1 1) plane was irradiated

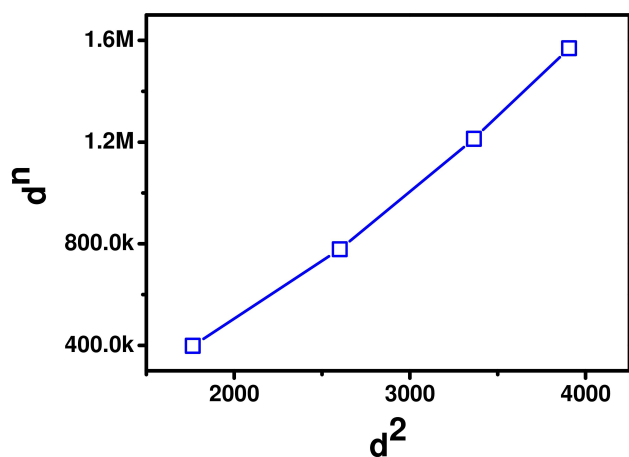


Figure 11. Plot of d^2 vs d^n of EDAPA crystal with (1 1 1) orientation

with a laser beam and the energy required to cause the catastrophic damage was measured using a power meter. The laser damage threshold of the grown crystals was evaluated using the expression Power Density (P) = $E/\tau_0 A$, where E - the energy required to cause damage (mJ), τ_0 - the pulse width (ns), A - area of the laser spot. The laser induced surface damage threshold of EDAPA crystal was estimated to be 9.1 GW/cm² and found to be higher than EDA(2,4)DNP (7.3 GW/cm²), urea (0.20 GW/cm²), benzimidazole (2.9 GW/cm²) and monohydrate piperazine hydrogen phosphate (4.0 GW/cm²) tested under similar experimental conditions.^[41,42] Higher laser induced damage threshold and lower the onset optical limiting threshold, wider will be the dynamic range of the materials, which is the most important requirement for OL based laser safety devices. EDAPA crystal with (1 1 1) orientation exhibit a wide dynamic range of 24.86 μ J/cm² – 9.1 GW/cm² making them the most potential material for fabrication of OL based laser safety devices against the most widely used Ti: Sapphire IR femto-second pulsed laser.

4. Conclusion

EDAPA single crystals grown by restricted solution growth technique exhibited well developed morphology with many habit faces and (2 0 0), (1 1 1) was identified to be the prominent plane of orientation. The detailed analysis of molecular structure was carried out using density functional theory calculations. First order hyperpolarizability of EDAPA (15.349×10^{-30} esu) was found to be 30 times that of urea and is due to the π -electron cloud movement from donor to acceptor which makes the molecule highly polarized. The performed calculations of the electronic and optical properties revealed certain peculiar features that can be suitable for the nonlinear optical applications. The performed first principles calculations of the electronic band structure showed EDAPA single crystals have HOMO (delocalized over both the ethylenediamine cations, -5.45 eV), LUMO (delocalized over the picrate anion, -2.27 eV) resulting a direct band gap of 3.18 eV. Z-scan measurements made with mode-locked Ti: Sapphire femtosecond near-IR laser pulses shows EDAPA crystal exhibit two-photon absorption and self-defocusing nature. It was shown that the studied crystals possess promising third-order optical susceptibilities, which allow to use the crystal as optical limiters. To clarify the origin of the observed effect, FMO and intensity dependent Z-scan studies was performed. It showed electrons cannot undergo one photon absorption due to the non-existence of energy states at 800 nm, 1.55 eV. So electrons in the HOMO (ground state, -5.45 eV) level absorbs two photons through simultaneous process and transit to the of LUMO level (excited state, 2.27 eV) of EDAPA crystal. Here energy gap of EDAPA crystal (3.18 eV) avails energy state to accommodate two photon absorbed excited electrons and thus the involved nonlinear absorption is ascertained to be genuine 2PA. Variation in the NLO coefficients arises due to the anisotropy of the crystal and here (1 1 1) orientation show almost one order of magnitude higher values than (2 0 0) plane. EDAPA crystal along (1 1 1) orientation which has high

nonlinear absorption coefficient (8.1×10^{-10} m/W) and wide dynamic range ($24.86 \mu\text{J}/\text{cm}^2 - 9.1 \text{GW}/\text{cm}^2$) can be a preferred candidate for high power optical limiting applications with ultrashort laser pulse (800 nm, 150 fs) excitation.

Conflict of Interest

The authors declare no conflict of interest.

Keywords: Organic NLO Crystal · Z-scan · Optical Limiting · Two-photon Absorption

- [1] R. L. Sutherland, *Handbook of Nonlinear Optics*, 2nd ed., Marcel Dekker, New York, 2010.
- [2] Y. R. Shen, *The Principles of Nonlinear Optics*, 1st ed., Wiley & Sons, New Jersey, 2003.
- [3] M. Saravanan, T. C. Sabari Girisun, G. Vinitha, S. Venugopal Rao, *RSC Adv.* **2016**, 6, 94, 91083–91092.
- [4] M. Domke, S. Wick, M. Laible, S. Rapp, H. P. Huber, R. Sroka, *J. Biophotonics*. **2018**, 11, 10, 1–23.
- [5] M. S. Bello-Silva, M. Wehner, C. De Paula Eduardo, F. Lampert, R. Poprawe, M. Hermans, M. Esteves-Oliveira, *Lasers Med. Sci.* **2013**, 28, 171–184.
- [6] W. J. Ertle, K. M. Donnelly, *Rockwell Laser Incident Database*. 2010.
- [7] P. K. Gupta, R. Hare, *Laser Physics and Technology, Springer Proceedings in Physics*. 1st ed., Springer, New York, 2012.
- [8] H. S. Nalwa, S. Miyata, *Nonlinear Optics of Organic Molecules and Polymers*, 1st ed., CRC Press, New York, 1997.
- [9] P. N. Prasad, D. J. Williams, *Introduction to Nonlinear Optical Effects in Organic Molecules and Polymers*, 1st ed., Wiley, New York, 1991.
- [10] L. Liu, C. He, H. Wang, Z. Li, S. Chang, J. Sun, X. Zhang, S. Zhang, *J. Mol. Struct.* **2011**, 989, 136–143.
- [11] M. Thangaraj, G. Ravi, T. C. Sabari Girisun, *Phys. B (Amsterdam, Neth.)*. **2014**, 449, 209–213.
- [12] M. Thangaraj, G. Ravi, T. C. Sabari Girisun, G. Vinitha, A. Loganathan, *Spectrochim. Acta, Part A*. **2015**, 138, 158.
- [13] C. Indumathi, T. C. Sabari Girisun, K. Anitha, S. Alfred Cecil Raj, *Opt. Mater.* **2016**, 60, 214–220.
- [14] C. Indumathi, T. C. Sabari Girisun, K. Anitha, S. Alfred Cecil Raj, *J. Phys. Chem. Solids*. **2017**, 106, 37–43.
- [15] C. Indumathi, T. C. Sabari Girisun, G. Vinitha, S. Alfred Cecil Raj, *J. Mol. Liq.* **2017**, 238, 89–95.
- [16] Fuks-Janczarek, R. Miedzinski, M. G. Brik, A. Majchrowski, L. R. Jaroszewicz, I. V. Kityk, *Solid State Sci.* **2014**, 27, 30–35.
- [17] M. Amalanathan, I. Hubert Joe, V. K. Rastogi, *Spectrochim. Acta, Part A*. **2013**, 108, 256–267.
- [18] C. F. Macrae, I. J. Bruno, J. A. Chisholm, P. R. Edgington, P. McCabe, E. Pidcock, L. R. Monge, R. Taylor, J. Van de Streek, P. A. Wood, *J. Appl. Crystallogr.* **2008**, 41, 466–470.
- [19] P. Seal, *ChemistrySelect*. **2017**, 2, 8393–8401.
- [20] P. Rawat, R. N. Singh, S. Sahu, P. Niranjana, H. Rani, R. Saxena, S. Ahmad, *ChemistrySelect*. **2016**, 1, 4008–4015.
- [21] D. R. Mohbiya, N. Sekar, *ChemistrySelect*. **2018**, 3, 1635–1644.
- [22] K. Fukuda, N. Matsushita, Y. Minamida, H. Matsui, T. Nagami, S. Takamuku, Y. Kitagawa, M. Nakano, *ChemistrySelect*. **2017**, 2, 2084–2087.
- [23] A. A. Bhagwat, N. Sekar, *ChemistrySelect*. **2018**, 3, 13654–13664.
- [24] N. N. Ayare, M. Rajeshirke, M. C. Sreenath, S. Chitrabalam, I. H. Joe, N. Sekar, *ChemistrySelect*. **2019**, 4, 3752–3761.
- [25] C. Adaikalaraj, S. Manivarman, *ChemistrySelect*. **2017**, 2, 10428–10434.
- [26] P. QingQing, G. Ping, D. Jiong, C. Qiang, L. Hui, *Chin. Sci. Bull.* **2012**, 57, 30, 3867–3871.
- [27] M. Karabacak, E. Yilan, *Spectrochim. Acta, Part A*. **2012**, 87, 273–285.
- [28] B. Kosar, C. Albayrak, *Spectrochim. Acta, Part A*. **2011**, 78, 160–167.
- [29] C. A. Mebi, *J. Chem. Sci.* **2011**, 123, 727–731.
- [30] E. Scrocco, J. Tomasi, *Adv. Quantum Chem.* **1978**, 103, 115–193.
- [31] F. J. Luque, J. M. Lopez, M. Orozco, *Theor. Chem. Acc.* **2000**, 103, 343–345.
- [32] M. Saravanan, T. C. Sabari Girisun, S. Venugopal Rao, *J. Mater. Chem. C*. **2017**, 5, 9929–9942.
- [33] M. Sheik-Bahae, A. A. Said, T. H. Wei, D. J. Hagan, E. W. Van Stryland, *IEEE J. Sel. Top. Quantum Electron.* **1990**, 26, 760–769.
- [34] C. Babeela, T. C. Sabari Girisun, *Opt. Mater.* **2015**, 49, 190–195.
- [35] V. N. Joshi, *Photoconductivity*, 1st ed., Marcel Dekker, New York, 1990.
- [36] B. Babu, J. Chandrasekaran, S. Balaprabakaran, P. Ilayabarathi, *Mater. Sci. –Pol.* **2013**, 31, 1, 151–157.
- [37] F. Pan, G. Knopfle, C. Bosshard, S. Follonier, R. Spreiter, M. S. Wong, P. Gunter, *Appl. Phys. Lett.* **1996**, 69, 1, 13–16.
- [38] N. Goel, N. Sinha, B. Kumar, *Opt. Mater.* **2013**, 35, 479–486.
- [39] B. R. Bijini, S. Prasanna, M. Deepa, C. M. K. Nair, K. Rajendra Babu, *Spectrochim. Acta, Part A*. **2012**, 97, 1002–1006.
- [40] K. Sangwal, *Mater. Chem. Phys.* **2000**, 63, 145–152.
- [41] T. C. Sabari Girisun, S. Dhanuskodi, *J. Cryst. Growth*. **2011**, 330, 43–48.
- [42] M. Saravanan, T. C. Sabari Girisun, S. Venugopal Rao, *J. Appl. Phys.* **2018**, 124, 193101–193111.

Submitted: September 1, 2019

Accepted: January 15, 2020